

# Hand and Finger Fracture Detection and Type Classification Using Image Processing

Mariam M Saii <sup>[1]</sup>, Ali M Mayya <sup>[2]</sup>

Professor Assistance <sup>[1]</sup> PhD <sup>[2]</sup>

Department of Computer Engineering

Tishreen University

Syria

## ABSTRACT

The current research introduces a novel method for fracture detection and classification. The basic stages of fracture detection includes preprocessing of bone image and morphological operations to obtain the ROI region which is manipulated by a post processing stage to remove non-fracture pixels. The suggested approach extract three features from bone image which are transverse, cracks and divergence features in order to define the fracture type or integrity of bone image.

The designed systems detect the different fracture types correctly beside the hybrid fracture type. We applied experiments on a dataset consisting of 155 bone images including 100 fracture images, 30 hand-fingers images and 25 normal images. The systems achieved 92% true detection rate for general bone fractures, 93.33% true detection rate for finger bone fractures and 93.33% true rejection rate. The experiments showed that the inner false detection rates between each type and the others are less than 4%.

**Keywords** :— Fracture Detection, Fracture Classification, Morphological Operations, Transverse Fracture, Spiral Fracture, Open Fracture.

## I. INTRODUCTION

Fracture detection is an important scope of recent medical image processing fields. The fracture is a break of any size [1] and can be caused by an accident or by other diseases.

There are three different types of fracture which are transverse, spiral, open and mixed fracture types [1]. Those types differs in some attributes and sometimes are caused by different factors. Transverse fracture is a break through the bone at a right angle to the long axis of the bone [2]. The transverse fracture is often caused by direct traumatic injury [1].

Spiral fracture is a highly unstable fracture that runs around the bone axis and caused mostly by a twist movement [1]. On the other hand, the open fracture or compound fracture is a broken bone in which an open wound exists. This fracture harms to the soft tissues of muscles and destroy some blood vessels [1].

Some of fracture especially in case of accidents many kinds of fractures exist together such as transverse and spiral, transverse and open or spiral and open.

Many research had been recently released and processed the problem of fracture detection. AL-AYYOUB et al. [3] detected fractures in long bones using x-ray images. They applied several steps on the bone image which were the preprocessing for noise reduction and image enhancement, feature extraction using edge detection and corner detection for the segmentation of bone regions. They also define other

advanced features such as texture detection and parallel edges. They applied their method on a dataset of 300 x-ray images consisting of 200 normal bone and 100 different bones fractures. They got, as a result, 83% detection precision and 90% for AUC. Their results were so promised but they limited their research in the long bones and did not define specifically types of detected fractures.

Anu T C et al. [4] also used the x-ray bone images for the detection of bone fracture. They applied several processing steps such as preprocessing, segmentation, edge detection, image feature extraction and classification into fracture and non-fracture regions. Their system has been tested on a set of images and got 85% for true detection rate but they did not declare the type and size of bone dataset.

Swathika et al. [5] used the morphological gradient for segmentation of bone. Their method computed the difference between dilation and erosion. After that, they subtracted the result image from the original one to get the gradient. The next steps were smoothing, dilation and canny edge detection. The researcher did not mention type and size of their databases.

In 2016, San Myint et al. [6] applied the canny edge detector to get the horizontal and vertical lines of x-ray bone images. They used Hough transform to extract features of edges and compute their numbers and angles in order to define the existence of fracture. They applied test on 21 x-ray images (including 5 normal images) of the lower leg bones and detected the fracture in 14 images correctly.

Gajjar et al. [7], as AL-AYYOUB et al., detected fracture in long bone images. They applied a preprocessing step in which images were smoothed by Gaussian filter and then computed the gradient magnitude using approximations of partial derivatives. At the next step, they computed the non-maxima suppression to the gradient magnitude and detected bone edges via a double thresholding techniques based on canny detector. The experiments were applied on 12 images and the researchers mention that the results were very accurate but they did not define that by numbers. The search did not take in account false rejection or false acceptance rates in case of normal bones; also, it did not define fracture types specifically.

Narayanaswamy et al. [8] applied preprocessing Gaussian filter to remove noise, then they separate the bone structure from the bone region. After that, Canny edge detector was applied and a Hough transform was used to detect fracture of a bone image. The result gave approximately 80% accuracy on a dataset consisting of 10 fracture images. The research, as many recent researches, did not take in account error rates in case of normal bones; also, it did not define fracture types.

Bhakare et al. [9] developed a method for bone fracture detection based on many steps which were the preprocessing, edge detection, segmentation, feature extraction and classification. In the classification step, they used many classifier such as K-NN, SVM and BPNN networks. Their system achieved 85% detection rate. They did not define neither the dataset specification nor the different classification under those different classifiers. Their work also did not take in account the classification of bone types, they satisfied with fracture detection only.

Recently, at 2018, Johari and Singh [10] designed a bone-fracture detection system. Their aim was to verify the accuracy of detection in x-ray images using canny edge detector. They applied the Gaussian filter to remove noise and canny detector to detect the horizontal and vertical lines. They found that Sigma 4.75 was the best match of Sobel edge threshold. There were many limitations of their approach. First, they used only one x-ray image to verify their approach and define the best threshold. They treated only one state of bone fracture, which is the transverse fracture; in addition, they did not define the accuracy or the value of enhancement they got.

Another studies at the field of medical and concrete image processing [11,12,13,14,15,16,17,18,19,20] were introduced from our previous studies at the same field. We used the most important algorithms including in those researches that have been based on the distance classifier, neural networks, feature extraction of medical images and preprocessing filtration.

Previous study at the field of fracture detection suffer from many limitations. The first one is the small size of dataset that led to less confidence of the system. Second, is that they did not take in account classification of fracture types. Third, is that some of them did not deal with normal conditions which means that their studies did not mention any thing about error

rates or acceptance rates. Our research tries to deal with all this concepts and process them correctly. The following sections will talk about our system description. After that, we will list our results and discuss them clearly.

## II. MATERIAL AND METHODS

The system branches into two embranchment, which are the general fracture detection and the finger fracture detection.

### A. System Description

#### A.1 General Fracture Detection:

The general fracture detection system consists of many steps in order to define the type of fracture. Those types are illustrated in figure 1

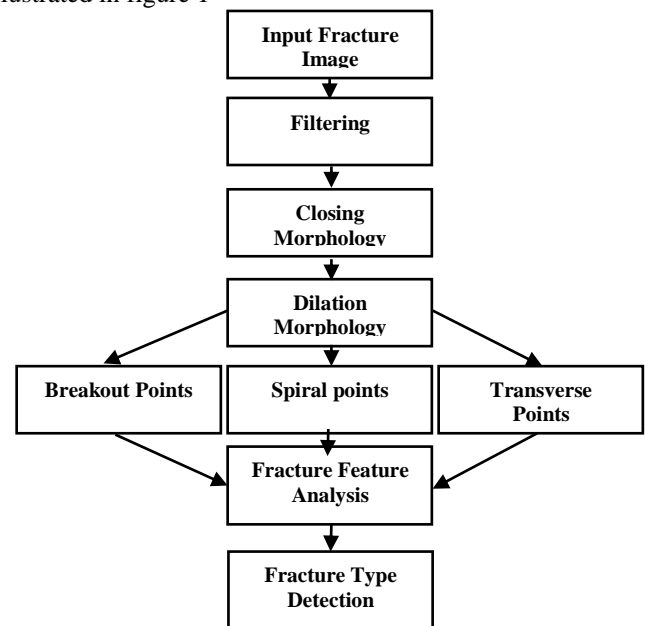


Figure (1). The steps of General Fracture Detection Method

There are four different types of general fracture which are transverse, spiral, open and mixed. The following steps are used to detect and classify these types.

Step 1. Read input image and transform it into grayscale (Figure (2-A)) to facilitate deal with one component rather than three.

Step 2. Filter the grayscale image using median filter (Figure (2-B)). The image is filtered by (3\*3) neighborhood mask to reduce the little changes into gray levels that are not fracture region.

Step 3. Transform the image into binary to deal with the binary form of the image (Figure (2-C)).

The next following steps are for detection of the three different fracture features (Transverse, Spiral and Open).

Step 4. Compute the Transverse Feature: Apply close morphological operation using an image as a structural element (SE). The image-based SE simulates the shape of transverse fracture. This step is called the fracture region detection step via modified template matching method which include the following sub-steps:

Step 4.1 Load a transverse template image which illustrated in figure (2,D).

Step 4.2 apply the close morphological operation on filtered image using the transverse template. This operation will affect the template-like regions which are the transverse-like fracture while the other regions wont affect. The result of closing is shown in figure (2,E).

Step 5. Compute The Spiral Cracks Feature: Apply the close operation on the grayscale filtered image via a binary SE (a disk with 10 point radius). This step aims to disguise the dark gray levels and obtain the bright ones. The spiral fracture is a dark crack into a bright gray levels. These regions will disappear after the close operation. With the subtraction of the original image and the close image we get the cracks region (spiral fracture region).

Step 6. Compute The Divergent Feature: Apply the open morphological operation on the grayscale filtered image via a binary SE (a disk with 4 point radius). This operation will illustrates the divergent points in image which indicates the open fracture regions.

Step 7. Detect the transverse regions:

Step 7.1 Subtract the binary image from the closed 4-step image to detect the regions with transverse-shape as shown in figure (2-F). the result image contains some little-area regions which are illuminated by calculating area of all regions and define the region with the biggest area (as in our previous studies [11,13]) (figure (2-G)).

Step 7.2 define the surrounding rectangle of the selected region from previous step and draw the corresponding coordinates on the original grayscale image to detect the fracture specifically.

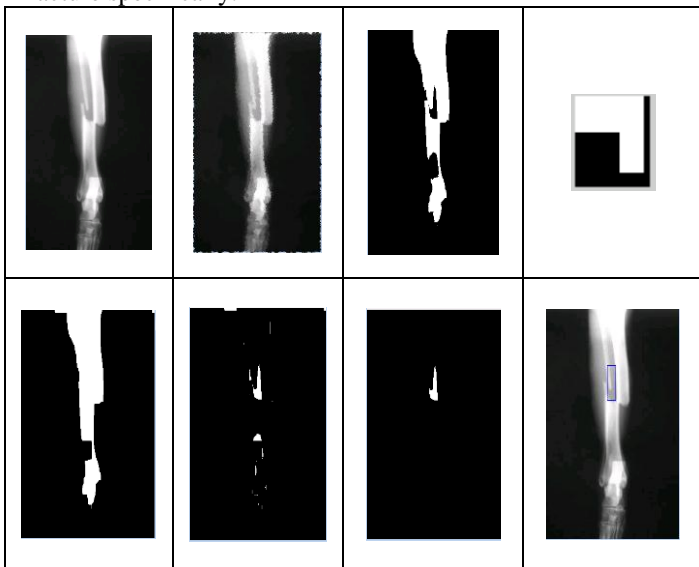


Figure 2. Transverse Fracture Detection Steps: (A) The original image, (B) The Filtered image, (C) The binary image, (D) The transverse-like template image, (E) The closing morphology of image D, (F) The subtraction result image, (G) The Biggest area of the subtraction result image, (H) The original image with surrounding rectangle on the transverse region

Step 8. Detect the spiral features:

The basic idea of detecting the spiral cracks is that cracks is a clue of spiral fracture. The closing image from step.5 which are the grayscale closed image is used in this step for the following scenario:

Step 8.a. subtract the original image from the closing image which the edges is faded and this will result in a difference image in which the edges is in a high contrast. These edges is the crack regions that we look for (figure (3-b)).

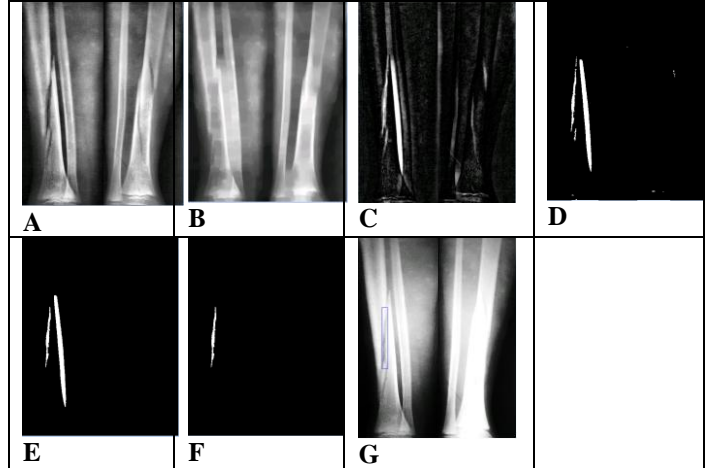


Figure 2. Transverse Fracture Detection Steps: (A) The original grayscale image, (B): The closing morphology of A, (C): The subtraction result, (D): The filtered image, (E): area open result, (F): the result of remove the false positive cracks, (G): The original image with surrounding rectangle on the crack region

Step 8.b. Transform subtraction image into a binary form (figure(2-c)).

Step 8.c. Remove the small-area regions and obtain the only the large regions which are the spiral cracks. The operation here is the opening process which illuminates the small regions with area less than 200 pixels.

Step 8.e. In some cases, the image still contain some outlier regions which are not cracks. In order to remove these pixels, we study a region property called "solidity" which is proportion of the pixels in the convex hull of the region that are also in the region. We define the spiral cracks from the fact that the spiral cracks have irregular shape and can be detected using the following solidity equation:

$$R(x,y) = \begin{cases} 0 & \text{if solidity} > 0.9 \\ 1 & \text{otherwise} \end{cases} \quad (1)$$

The equation.1 means that each region with solidity more than 0.9 will be illuminated, and as a result, only the cracks region remains.

Step 9. Detect the open (divergence) features:

In this step, we detect the divergence locations in the fracture region which is definitely open fracture regions. The following steps are the steps of open fracture:

Step 9.A. Take the opened image from step 6, and find the complement image to get the holes inside images which constitute via the open fracture. The result image (figure (3-c)) contains some extra outlier pixels which is illuminated via clear boarder operation.

Step 9.B. Compute the area and extent of each region (i.e. extent is the ratio of major axes length to the minor axes length [5,20]). To define the open fracture region we use the following equation:

$$F(x,y) = \begin{cases} 1 & \text{if } Extent(x,y) < 0.5 \ \& \ Area(x,y) > 50 \\ 0 & \text{otherwise} \end{cases} \quad (2)$$

The result image contains only the fracture region as illustrated in figure (3-D).

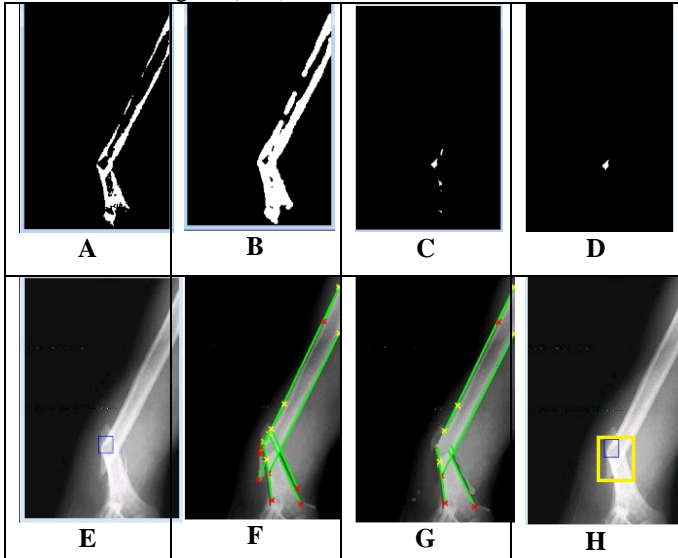


Figure 3. Open Fracture Detection: (A): Binary image from step 3, (B): The open operation of binary image, (C): Complement of image C, (D): Obtain the open region (E): The original image with surrounding rectangle on the crack region

Step 9.C. Compute the Hough transform of gray level image to compute lines that are on one straightness. The idea is that fracture contain more than two lines with one straightness, on the other hand the normal bone does not contain more than two lines. Figure (3-F) illustrates the result Hough lines.

Step 9.D. After the Hough transform has been applied, there is an extra step to delete the duplicate lines from Hough lines (in case of normal bone, there are some states in which the Hough transform result in many lines on the one straightness which must be deleted). Figure (3-G) shows the lines after delete the duplicated lines, and it can be noticed that there are more than two lines which indicates the open fracture.

Step 9.E. The double check step: The result of step 9.4 is fused with the result of the previous step 9.B because the step 9.B does not work for every open fracture and the step 9.C does not work for all open fracture states. The fusion of steps is done by "And" operator (i.e. if the step 9.D and step 9.E both indicate the existence of open fracture then the result is the "open fracture"). Figure (3-H) illustrates the fusion result that indicates without any doubt the existence of open fracture.

**A.2 Fracture Features Analysis:**

In this step, we took the three features which had been obtained from previous steps (Transverse feature, Divergence

Feature and Crack Feature). The next step was to define the fracture class based on those features which was detected using if-else rule as follows:

If Transverse feature==1 && Crack feature==0 && Divergence feature=0 type=Transverse  
 Else if Transverse feature==0 && Crack feature==1 && Divergence feature=0 type=Spiral  
 Else if Transverse feature==0 && Crack feature==0 && Divergence feature=1 type=Open.  
 Else Type="Normal".

**A.3 Finger Hand-Fracture Detection:**

The finger hand-fracture detection system consists of many steps illustrated in figure 4.

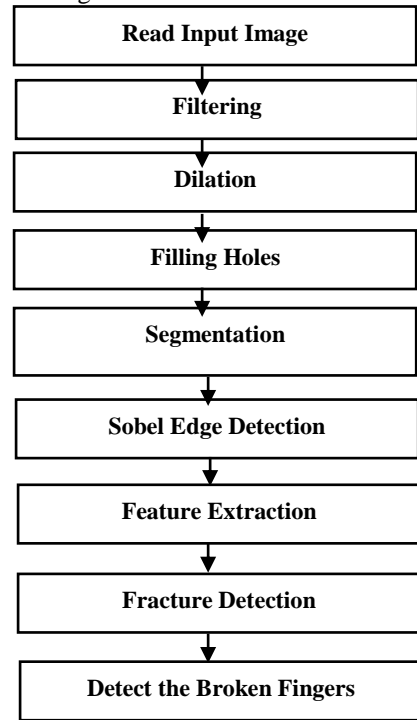


Figure 4. The steps of Finger Fracture Detection Method First, the input image is acquired and transform to the grayscale form and a smooth median filter with 3\*3 window is applied to get the result illustrated in figure (5-B).

The next step is the adaptive histogram equalization to distribute the gray levels over pixels and enhance the image's illumination (Figure (5-C)).

Third, the image is transformed into binary form using a high threshold 0.9 to get rid off background and preserve the bone region only, figure (5-D) illustrates the binarized image.

Filling holes operation is next applied to fill the gaps into the regions as figure (5-E) shows. After filling holes, closing morphological operation is done to get unified bone regions without any outlier points (Figure (5-F)).

The next step is the vertical edge detection process using Sobel vertical-edge detector with the famous mask [-1 0 1;-2 0 2;-1 0 1].

The basic step is then to define the degree of straightness of each vertical line to define the fracture (Figure (5-H)). If there is one line or more without one straightness, there will be fracture (Figure (5-G)).

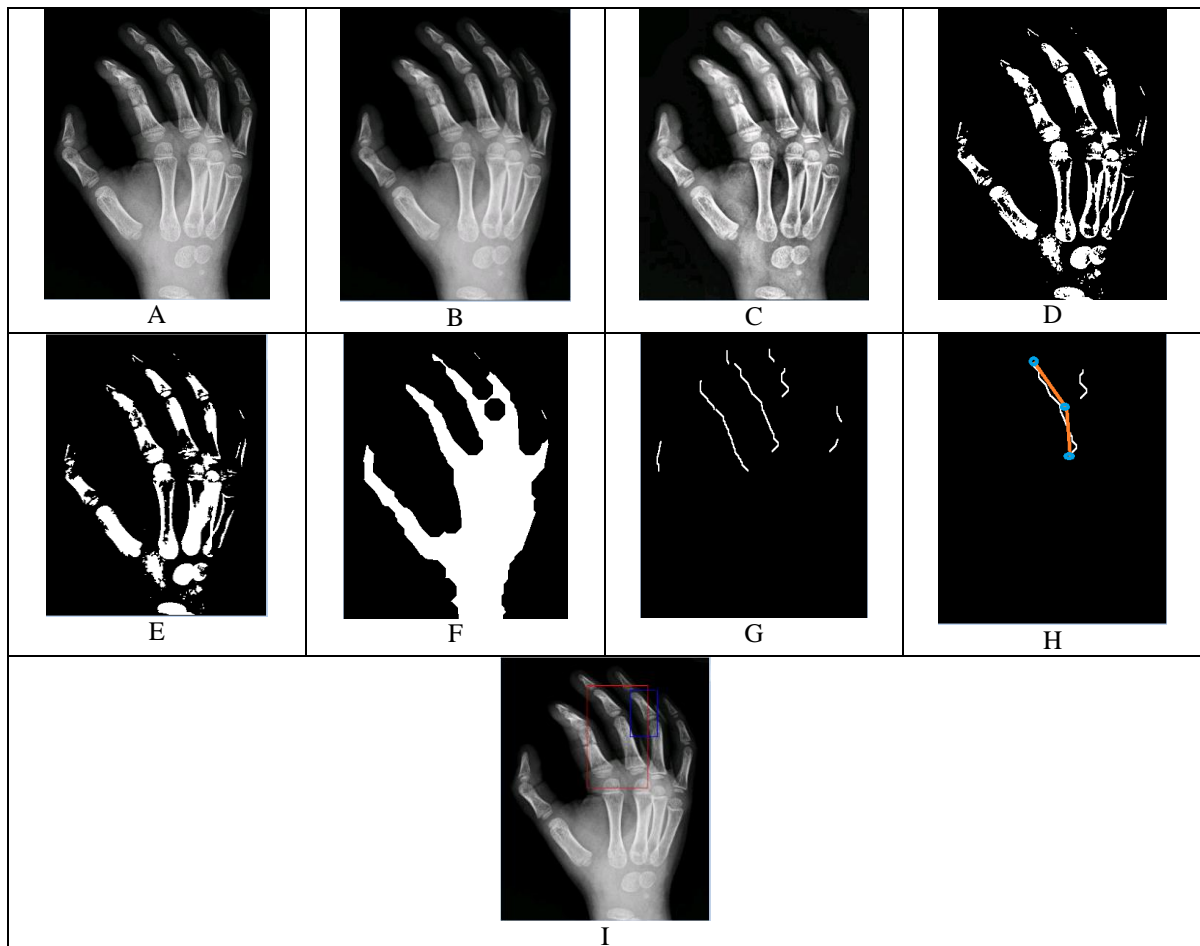


Figure 5. Steps of Detection Finger Fracture: (A): Original Image, (B): Median Filtered image, (C): Adaptive histogram equalization process, (D): Binarized image, (E): Filling Holes process, (F): Closing morphological process, (G): Vertical edges, (H): Detect degree of straightness of each vertical line, (I): Detect Finger Fracture.

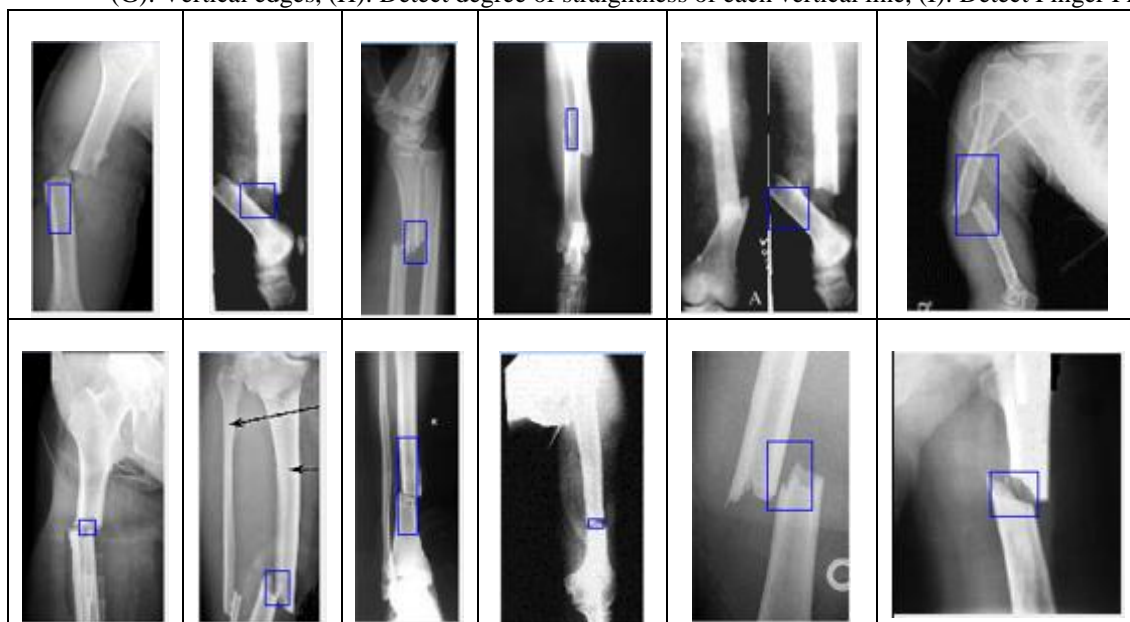


Figure 6. Some results of correctly transverse fracture detection

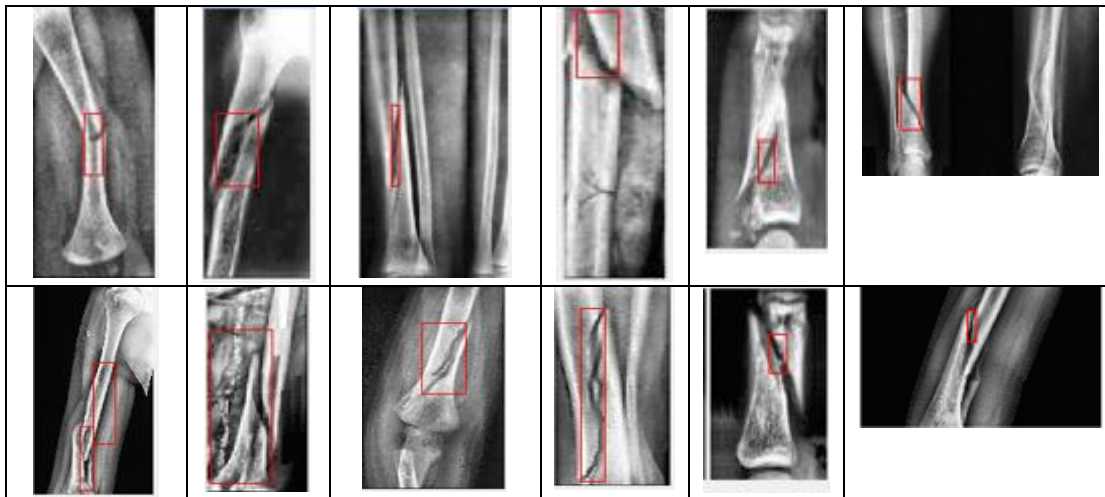


Figure 7. Some results of correctly Spiral fracture detection

### III. RESULTS AND DISCUSSION

We used a dataset consists of 155 bone images from different resources and different types. The images had been collected from Medical websites on Internet [21,22,23,24,25,26,27,28,29,30] and some local medical centres in our country. The images are jpeg and png formats and they are all grayscale.

#### A. General Fracture Detection Results::

We used 42 transverse fracture images and the system detect fracture in 40 samples with detection rate 95.23%. On the other hand, we used 38 spiral fracture image for the experimental process and the system detect fracture in 32 images with detection rate 84.21%. Figure 7 shows some of those detections. The last and least fracture type is the open fracture. We used 4 images and the system detect fracture in three of them as figure 8 illustrates.



Figure 8. Some results of correctly Open fracture detection

The last case of fracture detection is the mixed one in with there is more than one type of fracture. Figure 9 includes some of those cases and their detection results.

The system had been tested on the normal bone images to define the true rejection ability of the system. We used 15 images without any fracture type and the system reject the fracture existence in 14 of them with rejection rate 93.33%.

Table 1 concludes the previous results and gives an overview of the experimental process.

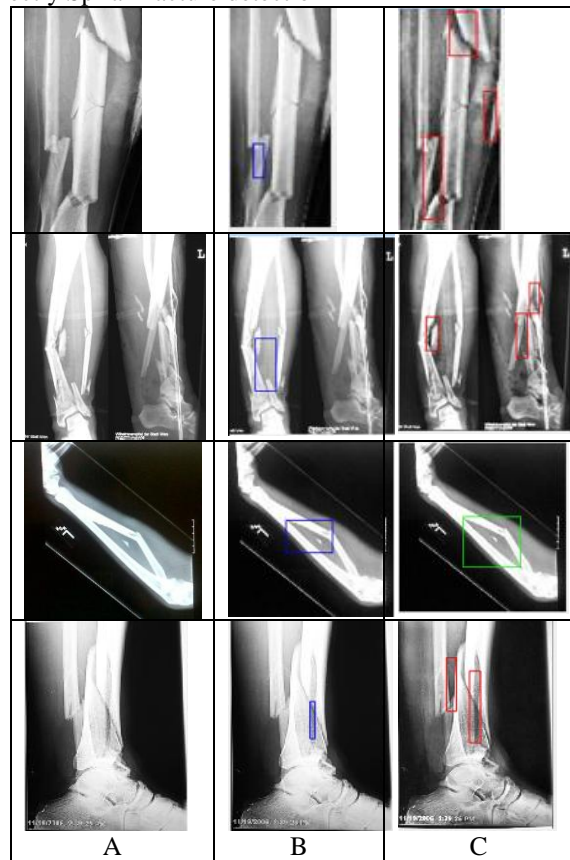


Figure 9. Some results of correctly Mixed fracture detection: (A) Original Image, (B and C) Fracture Detection

Table 1. The Detection and True Rejection rates

Type of Fracture	No. of Images	No. of Correctly Detection images	True Detection Rate	True Rejection on Rate
Transverse	42	40	95.23%	-
Spiral	38	35	92.1%	-
Open	5	4	80%	-
Mixed	15	13	80%	-
All	100	92	92%	-

Normal	15	14	-	93.33%
--------	----	----	---	--------

To define the robustness of our suggested system against false detections of wrong types of fracture, we detect situations in which the system gave extra detections corresponding to wrong fracture types (i.e. The system detected existence of spiral fracture and transverse fracture but the image contains only one of them).

False Detection Rate gives as the following equation:

$$FD=100*(\text{No. of Extra Detection images})/(\text{Total Number Of Images}) \quad (3)$$

Table 2. The False Detection across each type of fracture.

Type of Fracture	No. of Images	No. of Extra Detection images	False Detection Rate
Transverse	42	1	2.3%
Spiral	38	3	2.6%
Open	5	0	0%
Mixed	15	0	0%
All	100	4	4%

The result shows that the system achieved 92% detection rate for the hall fracture types and no less than 80% for the individuals. The system shows a good robustness as it achieved 93.33% true rejection rate for the normal situations and 4% false rejection rate for the extra detections.

**B. Finger Fracture Detection Results:**

For the finger-fracture detection system, thirty finger fracture images had been used and the system detect fracture in 28 samples with true detection rate 93.33%. The system also tested on 10 normal finger images and got 90% true rejection rate.

Figure 10 includes examples of true detection and true rejection samples of finger images.

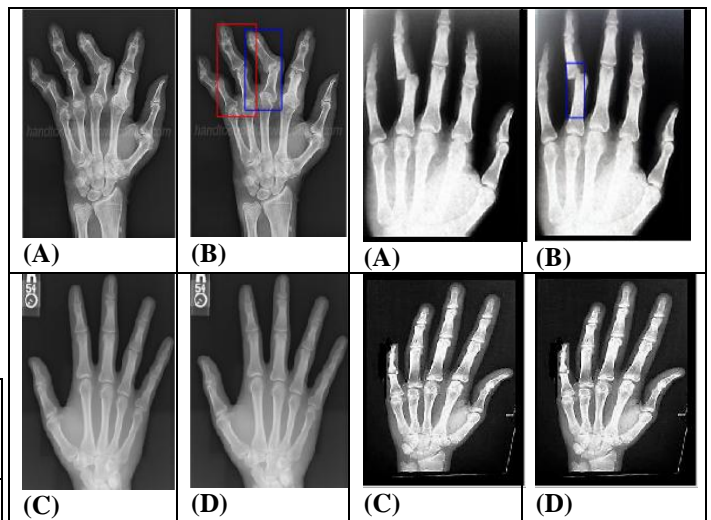


Figure 10 Examples of true detection and true rejection samples of finger images: (A,C) Original Image, (B,D) True Fracture Detection and Rejection Rate.

Table 3. Results of finger-fracture detection.

Type of Fracture	No. of Images	No. of Correctly Detection images	True Detection Rate	True Rejection Rate
Finger Fracture	30	28	93.33%	-
Normal Fingers	10	10	-	100%

The result illustrates that the finger-fracture detection system achieved 93.3% detection rate. The system shows a good robustness as it achieved 100% true rejection rate for the normal situations.

Most of fracture detection algorithms did not take in account all fractures types nor the rejection of false detections or false extra detections. Table 4 includes full comparative between our method and other ones at the same field.

Table 4. Comparison of most recent similar approaches and current study.

Researcher& Date	Methods	Database Size	Detection Rate	Classify types?	Error rate or TRR
AL-AYYOUB et al. [3] 2013	Edge detection, texture detection and parallel edges	300 (200 normal, 100 fracture)	83%	No	AUC: 90%
Anu T C et al. [4] 2015	Laplacian Gradient, K-means clustering	Not defined	85%	No	-
Swathika et al. [5] 2015	Morphological Gradient, Smoothing, Canny Detector	Not defined	Not defined	No	-
Myint et al. [6] 2016	Canny Detector	21 (16 Normal, 5	87.5%	No	-

		Normal)			
Gajjar et al. [7] 2017	Gaussian Filter, Gradient Magnitude, Canny Detector	12 images	Not defined	No	-
Narayanaswamy et al. [8] 2017	Canny edge detector, Hough Transform	10 miages	80%	No	-
Bhakare et al. [9] 2017	K-NN, SVM and BPNN	Not defined	85%	No	-
Johari and Singh [10] 2018	Gaussian filter, canny edge detector, Sobel Threshold	Not defined	Not defined	Transverse fracture only	-
<b>Current Research</b>	Morphological operations, Special Bone Feature Extraction, Sobel Edge Detection.	155 images (100 fracture images, 30 hand finger images, 25 normal images)	92% for general fracture, 93.33% for finger	Transverse, Spiral, Open, Hybrid, Fingers	Less than 4% inner error rate, 93.33% TRR

#### IV. CONCLUSION

In this paper, we introduced a full automatic fracture bone detection and classification method. We used many known tools of images processing such as morphological operations, edge detectors and hough transform, but the new steps were in the feature extraction step in which we extract the transverse, cracks and divergent features in order to define the fracture type specifically which did not treated as it should at other studies. We also developed another algorithm of finger fracture detection. We applied experiments on a dataset consisting of 155 images including 25 normal conditions. The system shows good robustness and assurance. We got less than 4% error rates, more than 90% true detection rates in both general and finger detection systems and 93.33% true rejection rate. In the next study, we aim to classify the types of fractures in all bone of the body.

#### REFERENCES

- [1] Donnelley M, Bone anatomy, PhD Thesis, Computer Aided Long-Bone Segmentation and Fracture Detection ,Chapter2: Fractures visualization and data collection, School of Computer Science, Engineering and Mathematics, (2008).
- [2] <https://www.medicinenet.com/script/main/art.asp?articlekey=8081>
- [3] Al-Ayyoub, M. and Al-Zghool, D., Determining the type of long bone fractures in x-ray images. WSEAS Transactions on Information Science and Applications, 10(8), (2013) 261-270.
- [4] Anu, T.C. and Raman, M.M.R., Detection of bone fracture using image processing methods. International Journal of Computer Applications (0975–8887), (2015) 6-8.
- [5] Swathika.B, Anandhanarayanan.k, Baskaran B., Govindaraj R., Radius Bone Fracture Detection Using Morphological Gradient Based Image Segmentation Technique, International Journal of Computer Science and Information Technologies, 6 (2), (2015) 1616-1619.
- [6] Myint, S., Khaing, A.S. and Tun, H.M., Detecting leg bone fracture in x-ray images. Int. J. Sci. Technol. Res, 5, (2016) 140-144.
- [7] Gajjar, B., Patel, S. and Vaghela, A., Fracture detection in X-ray images of long bone, (2017) 129-133.
- [8] Narayanaswamy G, Bindu A., Automatic Fracture Detection in Bone Images, International Conference on Signal, Image Processing Communication and Automation, (2017) 1-4.
- [9] Dhiraj B. Bhakare, Prajwal A. Jawalekar, Sumit D. Korde, A Novel Approach for Bone Fracture Detection Using Image Processing, International Research Journal of Engineering and Technology, 5(2), (2018) 193-195.
- [10] Johari, N. and Singh, N., Bone Fracture Detection Using Edge Detection Technique. In Soft Computing: Theories and Applications, Springer, Singapore, (2018) 11-19).
- [11] Mayya AM (2016) Human recognition based on ear shape images using PCA-Wavelets and different classification methods. Med Devices Diagn Eng: DOI: 10.15761/MDDE.1000103.
- [12] Ali M Mayya , Dr. Mariam M Saii . "Hybrid Recognition System under Feature Selection and Fusion". International Journal of Computer Science Trends and Technology (IJCT) V5(4):



- Page(78-84) Jul - Aug 2017. ISSN: 2347-8578. [www.ijcstjournal.org](http://www.ijcstjournal.org). Published by Eighth Sense Research Group.
- [13] Ali M Mayya , Mariam Saii . "Iris and Palmprint Decision Fusion to Enhance Human Recognition". International Journal of Computer Science Trends and Technology (IJCT) V5(5): Page(42-46) Sep - Oct 2017. ISSN: 2347-8578. [www.ijcstjournal.org](http://www.ijcstjournal.org). Published by Eighth Sense Research Group.
- [14] Mayya, Eng. Ali M and Dr. Mariam M Saii. "Hybrid Recognition System under Feature Selection and Fusion." (2017).
- [15] Mayya, Ali M., and Mariam Saii. "Iris and Palmprint Decision Fusion to Enhance Human Recognition.", 2017.
- [16] Segmentation, Iris. "IRIS RECOGNITION BASED ON WEIGHTING SELECTION AND FUSION FUZZY MODEL OF IRIS FEATURES TO IMPROVE RECOGNITION RATE." (2016), pp:2664-2680.
- [17] Ali Mamoud Mayya, "Different illumination, rotation and position invariant palm print segmentation", Joint Event on 5th International summit on Medical Biology & Bioengineering & 8th International Conference & Exhibition on Biosensors and Bioelectronics, J Bioengineer & Biomedical Sci, 7(4), DOI: 10.4172/2155-9538-C1-018, 2017.
- [18] Mayya AM, Saii M, (2016) Human recognition based on ear shape images using PCA-Wavelets and different classification methods. Med Devices Diagn Eng: DOI: 10.15761/MDDE.1000103.
- [19] Ali Mayya, Mariam Saii, "Evaluation of Features Selection in Enhancing the Performance of Palm Print Recognition", Al-Ba'ath University Journal, Vol(38), Issue(21), pp:95-120, 2016.
- [20] Mariam Saii, Ali Mia, Lung Detection and Segmentation Using Marker Watershed and Laplacian Filtering, International Journal of Biomedical Engineering and Clinical Science. Vol. 1, No. 2, 2015, pp. 29-42. doi: 10.11648/j.ijbecs.20150102.12.
- [21] <https://radiologykey.com/tibial-and-fibular-shafts>
- [22] <http://lermagazine.com/article/oa-after-ankle-fracture-surgerys-complex-role>
- [23] <https://www.orthobullets.com/trauma/1040/femoral-shaft-fractures>
- [24] <http://buyxraysonline.com/shop/normal-leg-2/>
- [25] <http://venturefortho.blogspot.com/2013/03/the-signal.html>
- [26] <https://radiopaedia.org/play/9010/entry/138192/case/22120/studies/22125>
- [27] <https://synapse.koreamed.org/search.php?where=avi&id=10.4055/jkoa.2008.43.5.651&code=0043JKOA&vmode=PUBREADER>
- [28] <https://www.orthobullets.com/trauma/1016/humeral-shaft-fractures>
- [29] <http://boneandspine.com/radiographs-of-tibia-and-fibula-fracture/>
- [30] <https://www.pinterest.com/pin/27936460161241422/>